engineering proceedings

MDPI

Proceeding Paper

Electrode Thickness Optimization in Color-Selective Inkjet-Printed Photosensitive Organic Field-Effect Transistors †

Christoph Steger [1,2,*], Ali Veysel Tunc [1,2], Christian Rainer [1,2], Ozan Karakaya [1,2], Dario Mager [3], Luis Ruiz Preciado [1,2], Trudi-H. Joubert [4], Uli Lemmer [1,2,3] and Gerardo Hernandez-Sosa [1,2,3,*]

1 Light Technology Institute, Karlsruhe Institute of Technology, Engesserstr. 13, 76131 Karlsruhe, Germany
2 InnovationLab, Speyererstr. 4, 69115 Heidelberg, Germany
3 Institute of Microstructure Technology, Karlsruhe Institute of Technology, Hermann-von-Helmholtz-Platz 1, 76344 Eggenstein-Leopoldshafen, Germany; dario.mager@kit.edu
4 Department of Electrical, Electronic and Computer Engineering, University of Pretoria, Private Bag X20 Hatfield, Pretoria 0028, South Africa
* Correspondence: steger.christoph@protonmail.com (C.S); gerardo.sosa@kit.edu (G.H.-S.)
† Presented at the Micro Manufacturing Convergence Conference, Stellenbosch, South Africa, 7–9 July 2024.

Abstract

This work introduces a general solution for printing wavelength-selective bulk-heterojunction photosensitive organic field effect transistors (PS-OFETs) by addressing electrode thickness variation and the feasibility of color selectivity in detecting incident light. The inkjet-printed silver electrode thickness was varied from 125 to 950 nm by multilayer printing. PIF, IDFBR, and ITIC-4F were chosen as the active semiconductor materials with complementary optical absorption. Results indicate that PS-OFETs exhibit the best functionality at an electrode thickness of approximately 325 nm and an active material combination with PIF:IDFBR (1:1). For the 540 nm wavelength, a responsivity of 55 mAW^{-1} was obtained. This is four-fold higher than the photoresponse obtained at 700 nm.

Keywords: color-selective photodetector; photosensitive organic field effect transistors; printed electronics; organic bulk heterojunction

Academic Editor: Willem Perold

Published: 24 September 2025

Citation: Steger, C.; Tunc, A.V.; Rainer, C.; Karakaya, O.; Mager, D.; Preciado, L.R.; Joubert, T.-H.; Lemmer, U.; Hernandez-Sosa, G. Electrode Thickness Optimization in Color-Selective Inkjet-Printed Photosensitive Organic Field-Effect Transistors. *Eng. Proc.* **2025**, *109*, 18. https://doi.org/10.3390/engproc2025109018

1. Introduction

One of the cornerstones of modern organic-based technology is light detection, used in state-of-the-art optical communication [1–3], imaging and medical sensing systems [4–6] and advanced flexible display technology [7–9]. Organic Field-Effect Transistors (OFETs) are at the forefront of organic electronics research, and the development of organic semiconductor devices is essential for many optoelectronic applications, including light-emitting diodes and transistors, such as OFET-driven photonics [10]. Recent advancements in OFET technology have focused on improving their performance, stability, and integration into various applications [11,12]. The successful integration of OFETs operating at low voltages, making them suitable for integration with low-power electronics and portable devices with flexible and stretchable substrates [13,14]. This has opened up new possibilities for innovative applications such as electronic skin [15,16], expanding biosensor technology [17] and the new generation of radio-frequency-identification (RFID) tags [18,19]. For an ideal optical sensor, it is necessary that the device be cost-effective and versatile enough to be fabricated on the desired substrate while taking advantage of the benefits of organic semiconductors, such as lightness, transparency and their optical properties [20].

2. Materials and Methods

Active layer preparation: Three different polymer inks were prepared for the active layers. One ink was prepared using the base material pristine polyindenofurorene-8-triarylamine (PIF; Merck, Darmstadt, Germany), acting as a transparent wide-bandgap polymer donor by diluting it in chlorobenzene at a concentration of 20 gL^{-1}. Blends were prepared prior to deposition. Both blends were made by dilution of 20 gL^{-1} of PIF and 20 gL^{-1}, of the respective complementary polymers IDFBR (NFA012; 1-Material Inc., Dorval, QC, Canada) and ITIC-4F (NFA014; 1-Material Inc., Dorval, QC, Canada) in chlorobenzene. All three inks were subjected to magnetic stirring in a nitrogen-filled glove box for at least 24 h. The materials were spin coated on glass substrates, each cleaned with acetone and isopropanol in an ultrasonic bath for at least 10 min.

Device preparation: The OFET devices were prepared on glass substrates cut to the size of 25 × 25 mm and a height of 1.2 mm. They were subjected to a cleaning procedure with acetone, followed by isopropanol in a sonic bath for 10 min. Subsequently, they were treated with Argon (Ar) plasma cleaning for 5 min inside a vacuum plasma oven. Figure 1 shows the variation in thickness as a function of the number of layers printed. 125 and 325 nm were achieved by single-layer, 750 nm by double-layer and 950 nm by triple-layer printing. For the structure shown in Figure 2a, the drain and source electrodes of varying thicknesses were deposited via multilayer inkjet printing with an P50 PiXDRO printer (SÜSS MicroTec SE, Garching, Germany) using silver dispersion ink (Silverjet DGP-40LT-15C; Sigma-Aldrich, St. Louis, MO, USA) and annealed on a hotplate at 120 °C for 30 min. The active layers were deposited via spin coating on top of the electrodes and cured for 30 min at 120 °C on a hotplate inside a nitrogen-filled glovebox. DPX-C (dichloro-di-para-xylylene; SCS, Indianapolis, IN, USA) was deposited as a dielectric with a Labcoater 2, Parylene Deposition Unit Model PDS 2010 (Specialty Coating Systems, Inc., Indianapolis, IN, USA), aiming for a thickness of 750 nm. Figure 2b shows the devices after finalizing them by thermal evaporation of a 100 nm thick silver layer through a mask to form the gate electrode.

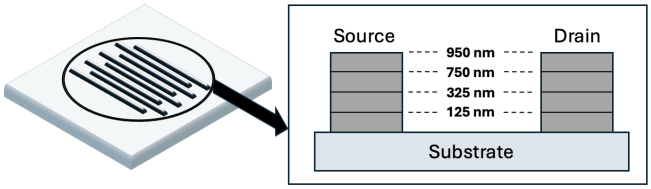

Figure 1. Schematic visualization of multilayered electrode thicknesses.

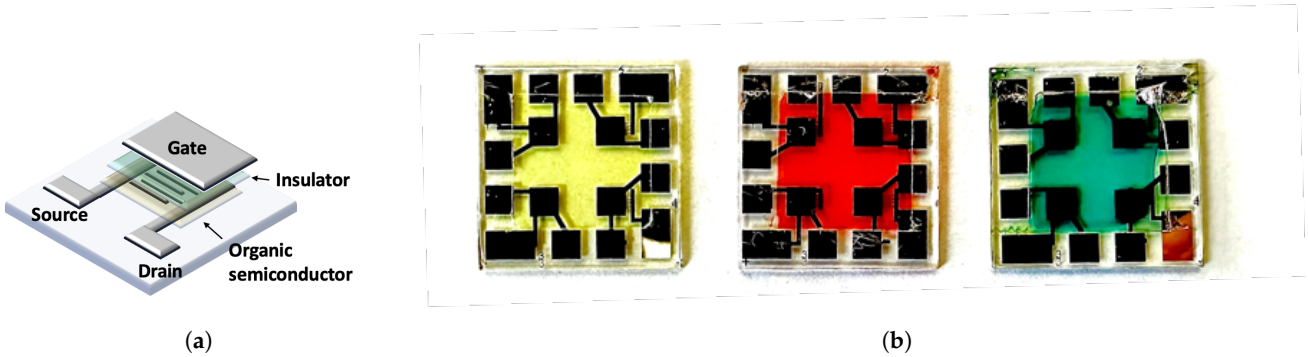

Figure 2. (**a**) Schematic structure of a single OFET device. (**b**) Finalized OFET devices (four OFETs per sample): transparent (PIF), red (PIF:IDFBR(1:1)) and blue (PIF:ITIC-4F(1:1)).

Device characterization: Electrode thicknesses were measured with a profilometer (Veeco Dektak 150; Veeco, Plainview, NY, USA). Current–voltage (I–V) characteristics were measured using a semiconductor parameter analyzer 4155C (Agilent, Santa Clara, CA, USA)

under ambient atmosphere. The same parameter analyzer was used to apply bias voltages for measurements of the spectral responsivity. A 450 W Osram XBO Xenon discharge lamp (Osram, Munich, Germany) served as a broad spectrum light source, which was filtered with a monochromator (Acton SP-2150i; Princeton Instruments, Trenton, NJ, USA). The UV–vis measurements were recorded using a AvaSpec-ULS3648 spectrometer (Avantes, Apeldoorn, The Netherlands) and a light source ranging from 300 to 1100 nm.

3. Results

Figure 3 shows the photoelectric properties of the fabricated devices with the mean values over the mentioned variations of electrode thickness: 125, 325, 750, and 950 nm.

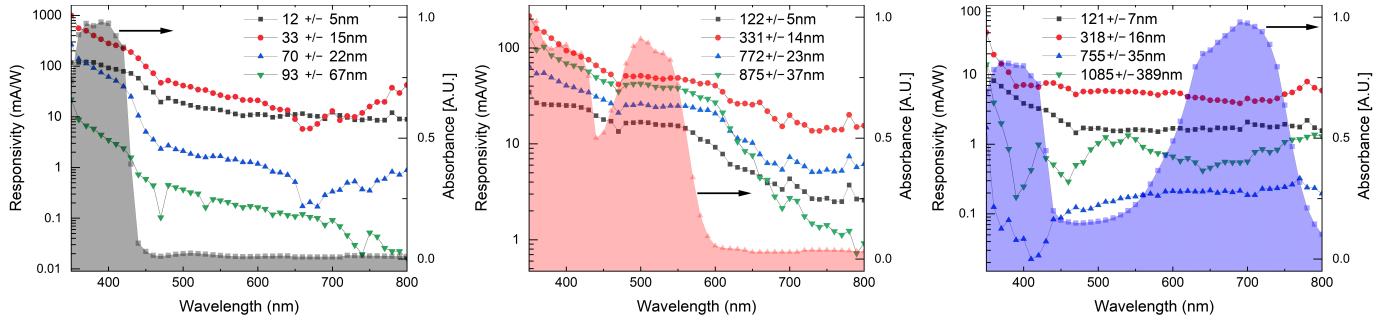

(**a**) (**b**) (**c**)

Figure 3. Spectral responsivity on the left axis (mAW^{-1}) and absorbance (shaded) on the right axis normalized to 1 (A.U.) of (**a**) PIF devices over the visual spectrum at $V_G = -50$ V and $V_D = -50$ V, (**b**) PIF:IDFBR(1:1) devices over the visual spectrum at $V_G = -50$ V and $V_D = -50$ V, and (**c**) PIF:ITIC-4F(1:1) devices over the visual spectrum at $V_G = -50$ V and $V_D = -50$ V. The four curves are represented by the electrode thicknesses investigated.

4. Discussion

Both PIF and PIF:IDFBR (1:1) materials exhibited the desired current enhancement behavior in the bandwidths where they have their highest absorption values. PIF, which has its absorption peak between 350 and 430 nm, presents a profile of currents and responsivity according to its absorption. As an example, for the 350 nm thick devices, at the 410 nm wavelength, the responsivity increases to up to 400 mAW^{-1}, whereas at higher wavelengths, where the absorption goes nearly to zero, the responsivity drops to around 5 mAW^{-1}.

The behavior of the PIF:IDFBR (1:1) follows a similar profile to those with PIF. The peak of interest is the IDFBR material being located between 470 and 550 nm. Within this spectral band, the devices show a noticeable increase in their responsivity, which, also taking the 350 nm thickness as the best example, is around 55 mAW^{-1}. At higher wavelengths, with the absorbance profile dropping from its peak to almost zero, the responsivity smoothly decreases to around 15 mAW^{-1}. These results seem to indicate that both materials have wavelength bands to which one can refer back based on the analysis of the optoelectronic measurements and therefore have color-selective characteristics.

Unlike the two materials discussed above, PIF:ITIC-4F (1:1) has good electronic output and transfer characteristics as a transistor but does not exhibit the expected optoelectronic behavior. PIF:ITIC-4F (1:1), with the absorption peak of interest being between 650 and 750 nm, shows a much lower photo-response. The responsivity trends towards a constant value of 5 mAW^{-1} along the whole measured spectrum, which does not allow to differentiate the wavelength of the incident light and therefore does not show color selectivity.

This technology should be explored on flexible substrates and by restricting the deposition of the active layer and gate electrode to inkjet printing in order to advance it toward manufacturing.

5. Conclusions

Electrode thickness of 325 nm achieves the maximal optoelectronic performance. In order to obtain sensors that can optically distinguish with high resolution, the polymers must have very fine absorption profiles that are ideally only noticeably greater than zero in the spectral bands in which the photosensitive OFET is intended to detect.

Author Contributions: Conceptualization, C.S. and A.V.T.; methodology, A.V.T., C.R. and L.R.P.; software, A.V.T., C.R., O.K. and L.R.P.; validation, A.V.T., T.-H.J. and G.H.-S.; formal analysis, C.S., A.V.T. and G.H.-S.; investigation, C.S. and A.V.T.; resources, G.H.-S. and T.-H.J.; writing—original draft preparation, C.S.; writing—review and editing, C.S. and A.V.T., C.R., D.M., T.-H.J. and G.H.-S.; visualization, C.S. and A.V.T.; supervision, A.V.T., G.H.-S. and T.-H.J.; project administration, D.M., T.-H.J. and G.H.-S.; funding acquisition, D.M., T.-H.J., G.H.-S. and U.L. All authors have read and agreed to the published version of the manuscript.

Funding: This work was financially supported by Deutsche Forschungsgemeinschaft (DFG, German Research Foundation) through grant HE 7056/6-1. G.H.S. thanks the DFG (Heisenberg-Professur, HE 7056/7-1) for the financial support. This research was co-funded by the South African Department of Science and Innovation Nano and Micro Manufacturing Facility grant.

Institutional Review Board Statement: Not applicable.

Informed Consent Statement: Not applicable.

Data Availability Statement: Additional data can be obtained from the authors.

Acknowledgments: The authors would like to thank the Baden-Württemberg Stiftung for facilitating the research collaboration between the Karlsruhe Institute of Technology and the University of Pretoria through the BWS+ Program.

Conflicts of Interest: The authors declare no conflicts of interest. The funders had no role in the research or in the decision to publish the results.

References

1. Suzuki, H. Organic light-emitting materials and devices for optical communication technology. *J. Photochem. Photobiol. Chem.* **2004**, *166*, 155. [CrossRef]
2. Lan, Z.; Lau, Y.S.; Cai, L.; Han, J.; Suen, C.W.; Zhu, F. Dual-Band Organic Photodetectors for Dual-Channel Optical Communications. *Laser Photonics Rev.* **2022**, *16*, 2100602. [CrossRef]
3. Zhu, Y.; Chen, H.; Han, R.; Qin, H.; Yao, Z.; Liu, H.; Ma, Y.; Wan, X.; Li, G.; Chen, Y. High-speed flexible near-infrared organic photodiode for optical communication. *Natl. Sci. Rev.* **2024**, *11*, nwad311. [CrossRef] [PubMed]
4. Khan, Y.; Han, D.; Pierre, A.; Ting, J.; Wang, X.; Lochner, C.M.; Bovo, G.; Yaacobi-Gross, N.; Newsome, C.; Wilson, R.; et al. A flexible organic reflectance oximeter array. *Proc. Natl. Acad. Sci. USA* **2018**, *115*, E11015–E11024. [CrossRef] [PubMed]
5. Murawski, C.; Gather, M.C. Emerging Biomedical Applications of Organic Light-Emitting Diodes. *Adv. Opt. Mater.* **2021**, *9*, 2100269. [CrossRef]
6. Lochner, C.; Khan, Y.; Pierre, A.; Arias, A.C. All-organic optoelectronic sensor for pulse oximetry. *Nat. Commun.* **2014**, *5*, 5745. [CrossRef] [PubMed]
7. Liu, K.; Ouyang, B.; Guo, X.; Guo, Y.; Liu, Y. Advances in flexible organic field-effect transistors and their applications for flexible electronics. *NPJ Flex. Electron.* **2022**, *6*, 1. [CrossRef]
8. Muccini, M. A bright future for organic field-effect transistors. *Nat. Mater* **2006**, *5*, 605–613. [CrossRef] [PubMed]
9. Qin, Z.; Gao, H.; Dong, H.; Hu, W. Organic Light-Emitting Transistors Entering a New Development Stage. *Adv. Mater.* **2021**, *33*, 2007149. [CrossRef] [PubMed]
10. Dey, A.; Singh, A.; Das, D.; Iyer, P.K. Organic Semiconductors: A New Future of Nanodevices and Applications. In *Thin Film Structures in Energy Applications*; Babu Krishna Moorthy, S., Ed.; Springer: Cham, Switzerland, 2015. [CrossRef]
11. Hong, K.; Yoon Yand, S.; Yang, C.; Se Hyun, K.; Choi, D.; Eon Park, C. Reducing the contact resistance in organic thin-film transistors by introducing a PEDOT:PSS hole-injection layer. *Org. Electron.* **2008**, *9*, 864. [CrossRef]
12. Waldrip, M.;Jurchescu, O.D.; Gundlach, D.J.; Bittle, E.G. Contact Resistance in Organic Field-Effect Transistors: Conquering the Barrier. *Adv. Funct. Mater.* **2020**, *30*, 1904576. [CrossRef]

13. Dey, A.; Singh, A.; Das, D.; Iyer, P.K. Photosensitive organic field effect transistors: The influence of ZnPc morphology and bilayer dielectrics for achieving a low operating voltage and low bias stress effect. *Phys. Chem. Chem. Phys.* **2016**, *18*, 32602–32609. [CrossRef] [PubMed]
14. Raj, B.; Kaur, P.; Kumar, P.; Gill, S.S. Comparative Analysis of OFETs Materials and Devices for Sensor Applications. *Silicon* **2022**, *14*, 4463–4471. [CrossRef]
15. Sokolov, A.N.; Tee, B.C.-K.; Bettinger, C.J.; Tok, J.B.-H.; Bao, Z. Chemical and Engineering Approaches to Enable Organic Field-Effect Transistors for Electronic Skin Applications. *Acc. Chem. Res.* **2012**, *45*, 361–371. [CrossRef] [PubMed]
16. Kyaw, A.K.K.; Loh, H.H.C.; Yan, F.; Xu, J. A Polymer Transistor Array with a Pressure-Sensitive Elastomer for Electronic Skin. *J. Mater. Chem. C* **2017**, *5*, 12039–12043. [CrossRef]
17. Niu, Y.; Qin, Z.; Zhang, Y.; Chen, C.; Liu, S.; Chen, H. Expanding the potential of biosensors: A review on organic field effect transistor (OFET) and organic electrochemical transistor (OECT) biosensors. *Mater. Futur.* **2023**, *2*, 042401. [CrossRef]
18. Gay, N.; Fischer, W.-J. OFET-Based Analog Circuits for Microsystems and RFID-Sensor Transponders. In Proceedings of the Polytronic 2007—6th International Conference on Polymers and Adhesives in Microelectronics and Photonics, Tokyo, Japan, 8 October 2007; pp. 143–148. [CrossRef]
19. Shen, S.; Sun, L.; Wang, R.; Gu, L. Simulation and Design of Organic RFID Based on Dual-Gate OFET. In Proceedings of the 2016 3rd International Conference on Information Science and Control Engineering (ICISCE), Beijing, China, 8–10 July 2016; pp. 1413–1416. [CrossRef]
20. Yamashita, Y. Organic semiconductors for organic field-effect transistors. *Sci. Technol. Adv. Mater.* **2009**, *10*, 024313. [CrossRef] [PubMed]